STEP-LIKE TEMPERATURE FLUCTUATIONS ASSOCIATED WITH INVERTED RAMPS IN A STABLE SURFACE LAYER

TOKIO KIKUCHI and OSAMU CHIBA

Faculty of Science, Kochi University, Kochi 780, Japan

(Received in final form 19 June, 1984)

Abstract. Ensemble averages of temperature before and after step-like temperature fluctuations reveal the presence of inverted ramps in a stable surface layer. Normalized frequency of upward steps increases with increasing stability, whereas normalized magnitude of the temperature step decreases with stability and becomes constant at about $R_f = 1$. These results suggest that the significance of temperature steps increases as stability increases. In moderate stability, the temperature pattern shows a gradual decrease after an upward step, which can be called a time-inverted ramp. Descending air and large downward heat flux are observed in a time-inverted ramp, suggesting a contribution from an ordered motion in wind. On the other hand, the temperature steps are related to gravity waves in strong stability.

1. Introduction

The presence of organized motion was first recognized in laboratory turbulence with the flow visualization technique (e.g., Kline *et al.*, 1967), and later, with the conditional sampling method (e.g., Wallace *et al.*, 1972). Since knowledge of detailed structure of turbulence will improve predictions of eddy diffusivities of momentum, heat, etc., it is desirable to investigate such organized structures in atmospheric turbulence.

A ramp-like feature of temperature fluctuations, which is evidence of organized structures, has been observed and investigated in the unstable atmospheric surface layer (e.g., Kaimal and Businger, 1970; Phong-anant *et al.*, 1980; Antonia *et al.*, 1979). Although the ramp is also found in stable conditions in an inverted form having a gradual decrease associated with a sharp increase in temperature (e.g., Kaimal, 1974; Phong-anant *et al.*, 1980), little is known about the 'inverted ramp' perhaps because the main concern has been with respect to normal ramps in unstable conditions and because only a few examples have been found by each worker.

In this paper, inverted ramps are investigated using surface-layer turbulence data obtained mainly in stable conditions and using an automatic detection scheme developed for this purpose.

2. Experiments

Surface-layer field experiment was carried out in a field at the Kochi University Farm using a vertical component sonic anemometer-thermometer (Kaijo Denki, DAT–100) at a height of 11 m, five three-cup anemometers (Makino, AC–750P) at heights of 1, 2, 5, 8, and 20 m and four copper-constantan thermocouple thermometers at heights of 3, 8, 11, and 20 m on a 20-m tower in December 1980 (Chiba and Kikuchi, 1982). The

Boundary-Layer Meteorology **31** (1985) 51–63. 0006–8314/85/0311–0051$01.95.

experimental field is about 250 × 500 m in size and the tower is located near the north-east corner of the farm (Chiba, 1984).

The outputs of the vertical wind fluctuation, w, and the temperature fluctuation, θ, from the sonic anemometer-thermometer were recorded with an FM cassette recorder (TEAC R–70A) and were played back later for sampling with an A/D converter controlled by a personal computer (TEAC/TANDY PS–80). Data were sampled at a rate of 20 Hz and were stored on digital cassette tapes.

A total of 81 runs of 20 min duration each were obtained during the observation period. As a stability index, Richardson number, R_i, at a height of 11 m was calculated from the wind and temperature profiles using a familiar formula, $R_i = (g/\Theta)(\partial\Theta/\partial z)/(\partial U/\partial z)^2 = (gz/\Theta)[\partial\Theta/\partial(\ln z)]/[\partial U/\partial(\ln z)]^2$. The logarithmic gradients, $\partial\Theta/\partial(\ln z)$ and $\partial U/\partial(\ln z)$ were calculated by using the least-square method. 59 runs were in stable conditions and 22 were in unstable conditions.

3. Detection Scheme for Temperature Steps

The method of conditional sampling has been used for investigating ordered structures of laboratory turbulence (e.g., Kovasznay *et al.*, 1970), atmospheric turbulence (Kahlsa, 1980; Antonia *et al.*, 1983), and temperature fluctuations (Phong-anant *et al.*, 1980). There are various methods for determining whether the data should be sampled or not. In laboratory turbulence, a sampling signal is often generated from some analog circuits such as filters and comparators. A similar method is used by Kahlsa (1980) for investigation of the fine structure of atmospheric turbulence.

On the other hand, for detection of relatively large structures such as temperature ramps, it is much easier, at first, to sample non-conditionally, then to select data according to some criteria relevant to the large structure considered. Phong-anant *et al.* (1980) used a graphic terminal and detected ramps by eye. However, it is more desirable that the detection be done automatically by computer, using digital filters and comparators; eye detection may lead to some error in the resulting ensemble average.

As noted by many workers, the ramp in unstable conditions is characterized by a gradual increase in temperature with time followed by a sharp decrease. On the other hand, Phong-anant *et al.* (1980) state that the temperature ramps during a stable period exhibited 'a gradual fall in temperature with time followed by a sharp increase'. In both cases, sharp changes (increase or decrease) appear in temperature traces and they can be called 'temperature steps'. Since it is easier to detect a sharp change rather than a gradual one, a scheme has been developed for detecting temperature steps.

A computational technique called digital filter can be used to remove high frequency noise and to determine a threshold level of detection. One method proposed by Saito and Ishii (1969) is used here for computing time and memory restriction; a low-pass recursive filter of the first order is written as

$$y_i = x_i + x_{i-1} - qy_{i-1}, \tag{1}$$

where x and y are the original and filtered values respectively, and q is the filter

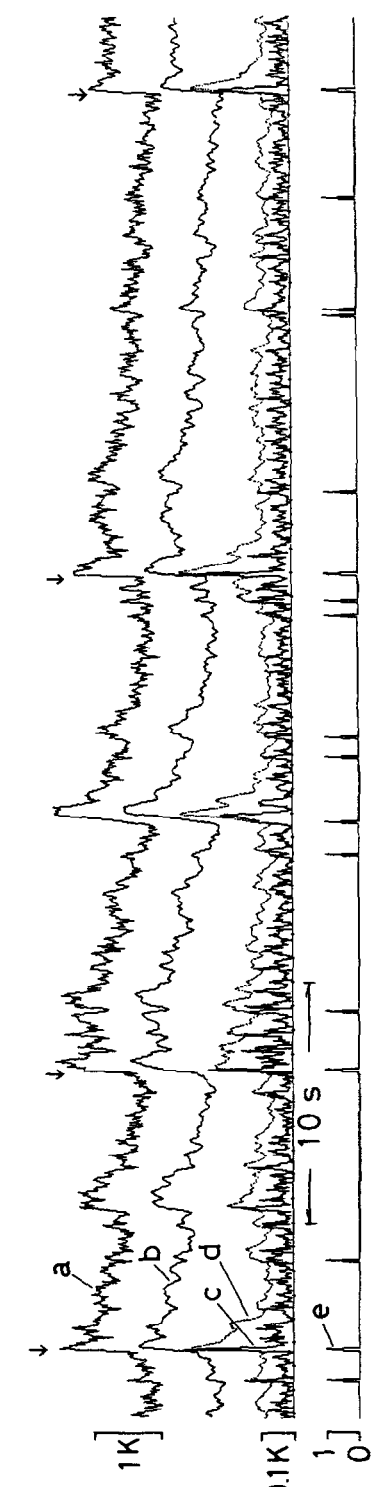

Fig. 1. Detection scheme of step-like variations associated with temperature steps. (a) Raw temperature data measured at $z = 11$ m. (b) Low-pass-filtered at 2.0 Hz. (c) Absolute values of differences θ' and (d) the threshold values $c\langle\theta'\rangle$ ($\langle\rangle$ denotes 0.4 Hz low-pass-filtered value). (e) Index function I. Note that two or more consecutive occurrences of $I = 1$ indicate a temperature step.

coefficient given by

$$q = -\cos 2\pi f\Delta t/(1 + \sin 2\pi f\Delta t), \tag{2}$$

where f is the cut-off frequency and Δt is the sampling interval.

Figure 1 illustrates the conditional sampling scheme used in this study. The raw signal of θ, which is indicated by (a), is low-pass filtered with a cut-off frequency of 2.0 Hz in order to eliminate spike-like fluctuations. The filtered trace is shown by (b). Then the absolute value of temperature difference, θ', is calculated between adjacent data points (0.05 s interval). The θ' signal is low-pass filtered at 0.4 Hz, which is denoted by $\langle \theta' \rangle$. If θ' is much larger than $\langle \theta' \rangle$, then a temperature step can be said to have occurred. Therefore, an indicator function I is defined as

$$I = \begin{cases} 0 & (\theta' < c\langle \theta' \rangle) \\ 1 & (\theta' \geq c\langle \theta' \rangle), \end{cases} \tag{3}$$

where c, the threshold coefficient, must be much larger than unity. In this study, a value of 3 is chosen for c after some trial and error. The traces of θ', $3\langle \theta' \rangle$ and I are shown by (c), (d), and (e), respectively. Appearance of a temperature step is defined as two or more consecutive appearances of $I = 1$, which is denoted by arrows; the criterion of consecutive appearances is used because I is rather sensitive to small fluctuations even though the filter and threshold coefficients are determined after trial and error.

4. Ensemble Averages of Temperature Associated with Upward and Downward Steps

In order to get a rough idea about the overall appearance of steps in both unstable and stable conditions, all the steps regardless of whether they were upward (cold-to-hot) or downward (hot-to-cold), were selected and ensemble average of temperature, $\hat{\theta}$, was

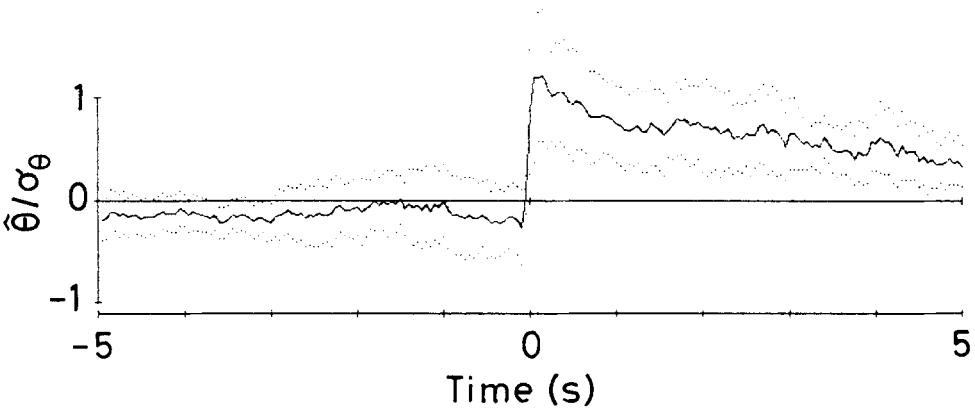

Fig. 2. An example of an ensemble average of temperature, $\hat{\theta}$, before and after the selected steps in a 10-s interval. Note that the resulting values are normalized with the root-mean-square σ_θ. Dots indicate the standard errors in the ensemble averages. Both upward and downward steps are sampled. $R_i = 0.97$.

calculated over a period of 5 s before and after the steps. Figure 2 shows an example of a conditionally averaged pattern associated with the temperature steps. In this example, a total of 61 steps were detected and the resulting pattern shows an upward step. If there were more downward than upward steps, the resulting pattern would be reversed.

A temperature step height, θ_s, is defined as the temperature difference between two instances where the time derivative of temperature changes its sign before and after the maximum absolute value of temperature derivative occurs. The sign of θ_s indicates whether upward or downward steps are predominant in the run. Figure 3 shows the relation between the temperature step height and the logarithmic temperature gradient, $\partial\Theta/\partial(\ln z)$. It is clear that the step is upward if the surface layer is stable, and vice versa, although some data points are scattered into the second and the fourth quadrants. The size of the square symbol in Figure 3 represents the number of steps detected in every

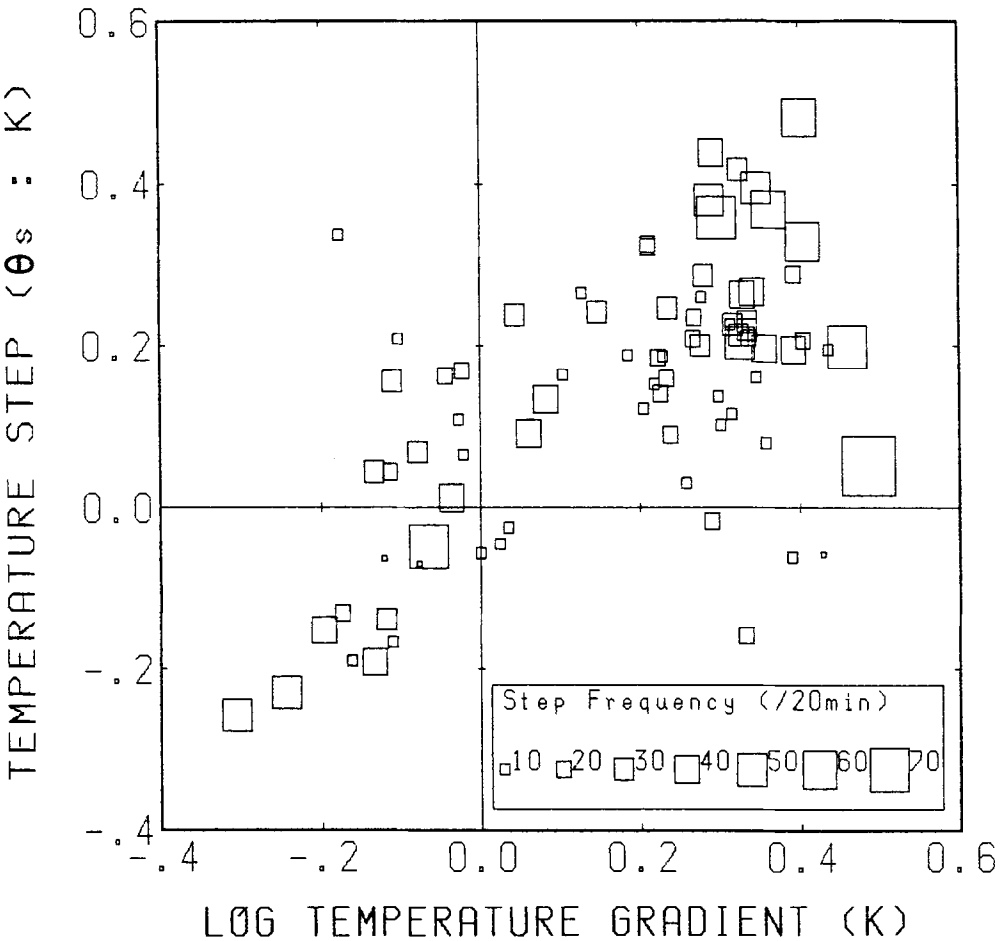

Fig. 3. The magnitude of a temperature step (θ_s) vs the logarithmic temperature gradient ($\partial\Theta/\partial(\ln z)$). The size of the square symbols shows the frequency of steps in a 20-min run. Both the upward and downward steps are sampled.

20-min run. It can be seen that the step frequency is high when there is a large temperature gradient.

5. Upward Steps in Stable Conditions

Downward steps are related to the temperature ramps in unstable conditions, and these have been studied extensively by many investigators. However, little is known about the upward steps with inverted ramps. Thus the runs in stable conditions were selected and re-analyzed using the same method as before, but only the upward steps were selected this time. Some runs with positive Richardson number were found to have upward heat flux, which is typical in unstable conditions, and these runs were excluded from the analysis because some nonstationary process is considered to be involved. In the

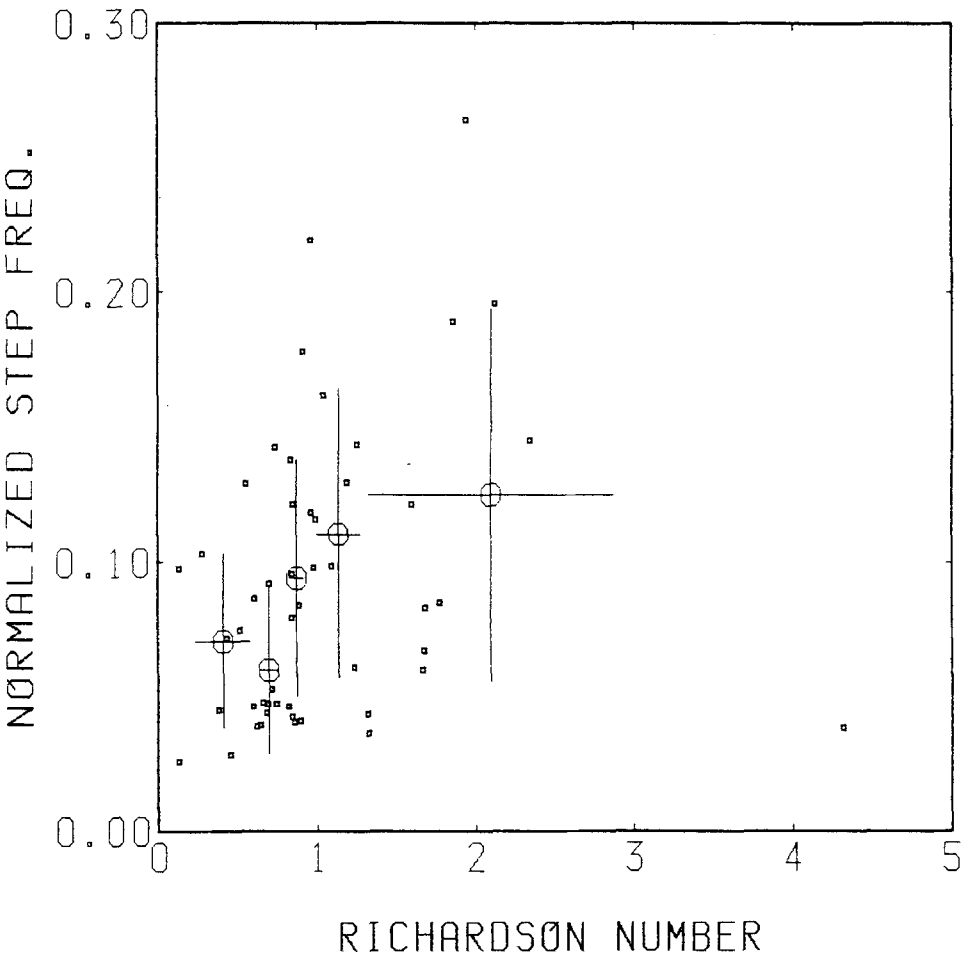

Fig. 4. Normalized frequency of upward steps, $f_s^{\uparrow} = n_s^{\uparrow} z/U$, where $n_s^{\uparrow}$ is the number of upward steps in a second, plotted against the Richardson number, R_f. Large symbols represent averages of 10 data points with bars for standard deviations.

following, the frequency and height of upward steps are normalized with appropriate parameters and plotted against Richardson number, R_i. Another frequently used stability parameter, z/L (L is the Monin-Obukhov length), is not used here because it diverges to infinity at the critical Richardson number in extremely stable conditions.

A normalized frequency of step, $f_s^{\uparrow}$ can be defined as

$$f_s^{\uparrow} = n_s^{\uparrow} z/U\,, \tag{4}$$

where $n_s^{\uparrow}$ is the number of steps in unit time. Equation (4) is analogous to the definition of a conventional normalized wave frequency. Figure 4 displays $f_s^{\uparrow}$ against R_i in stable conditions. The plotted data show considerable scatter, perhaps due to the simplified detection scheme, but it is evident from the averaged data points that the step appears more often at large stability. The data point at $R_i = 4.3$ is positioned at an exceptionally

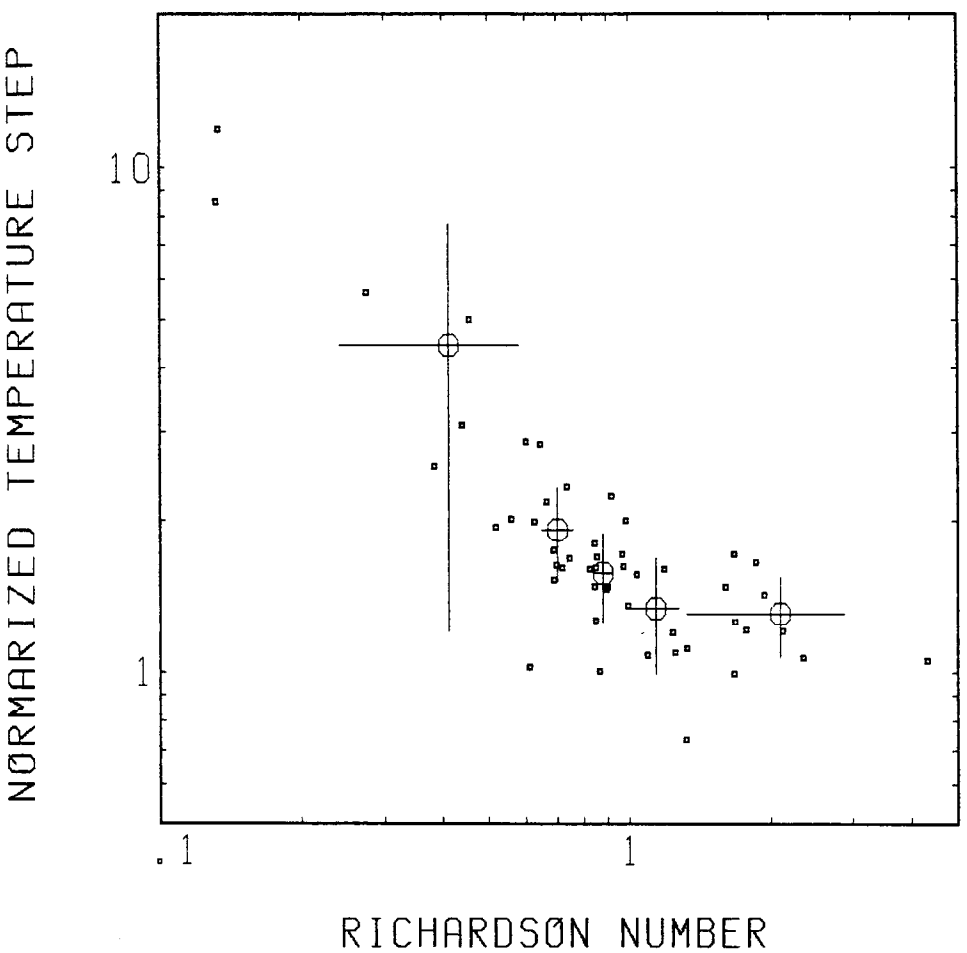

Fig. 5. Normalized upward temperature step, $\theta_s^{\uparrow}/[\partial\Theta/\partial(\ln z)]$, vs the Richardson number. Large symbols are the same as in Figure 4.

low frequency because the number of steps selected in 20 min is too small to determine meaningful statistics owing to the extremely low wind speed.

The frequency of step is expected to be related to the peak frequency of the temperature spectrum because both represent large-scale temperature fluctuations. The observed tendency agrees with the results of Kaimal *et al.* (1972) with respect to the logarithmic spectral peak frequency for θ.

Figure 5 shows the upward temperature step height, $\theta_s^{\uparrow}$, which is normalized with the logarithmic gradient of temperature, $\partial\Theta/\partial(\ln z)$, against R_i. The data are widely scattered, but the behavior of averaged values plotted by large symbols indicates that $\theta_s^{\uparrow}$ decreases with increasing R_i from near neutral to moderate stability ($0 < R_i \lesssim 1$) and reaches a constant value in strong stability ($1 \lesssim R_i \lesssim 4$).

The effect of the step seems to become significant as R_i reaches zero, but in near neutral conditions, small steps are concealed by turbulent fluctuations and cannot be detected with the present detection scheme. Therefore, it must be concluded that the step-like fluctuation becomes significant as the stability increases.

6. Shapes of the Inverted Ramps

Two kinds of ramps can accompany upward steps: one with a gradual fall before the step, and another with a gradual fall after it. In other words, the ordinary ramp pattern found in unstable conditions is inverted with temperature in the former case and with time in the latter. In order to determine which kind of inverted ramps is present in stable conditions, the slopes of the temperature trace before and after the ensemble-averaged step are compared.

Two stages associated with the temperature step are defined and are illustrated in the inset of Figure 6. Stage 1 starts at the instant when the difference from the minimum value is one-third of the temperature step height $\theta_s^{\uparrow}$ and ends when the temperature reaches its minimum value. Stage 2 begins at the instant of the temperature maximum and ends when the temperature becomes $(1/3)\theta_s^{\uparrow}$ smaller than the maximum. The ensemble averaging time (10 s) is sometimes insufficient for determination of the one-third point. In this case, the start point of Stage 1 or the end point of Stage 2 is chosen as the boundary of the ensemble average interval (5 s before or after the step).

The duration periods of Stages 1 and 2 are defined as t_1 and t_2, respectively; thus the slope of temperature in Stages 1 and 2 can be defined as $\theta_s^{\uparrow}/3t_1$ and $\theta_s^{\uparrow}/3t_2$, respectively. If the ramp is before the step, then $t_1 < t_2$, and vice versa. Figure 6 shows the ratio of the periods t_2/t_1 plotted against the Richardson number R_i. Some runs in which the frequency of step in 20 min is smaller than 10 are omitted from the figure because such data may yield unreliable information on the shape of the ramps.

Although the data contain considerable scatter, most of the values in moderate stability are below unity ($t_1 > t_2$). Therefore, the term 'inverted ramp' must be interpreted as ramp inverted with time. On the other hand, the duration of Stage 1 is shorter than that of Stage 2 at higher stability ($R_i > 1.5$), which means that the ramps are inverted with temperature rather than with time.

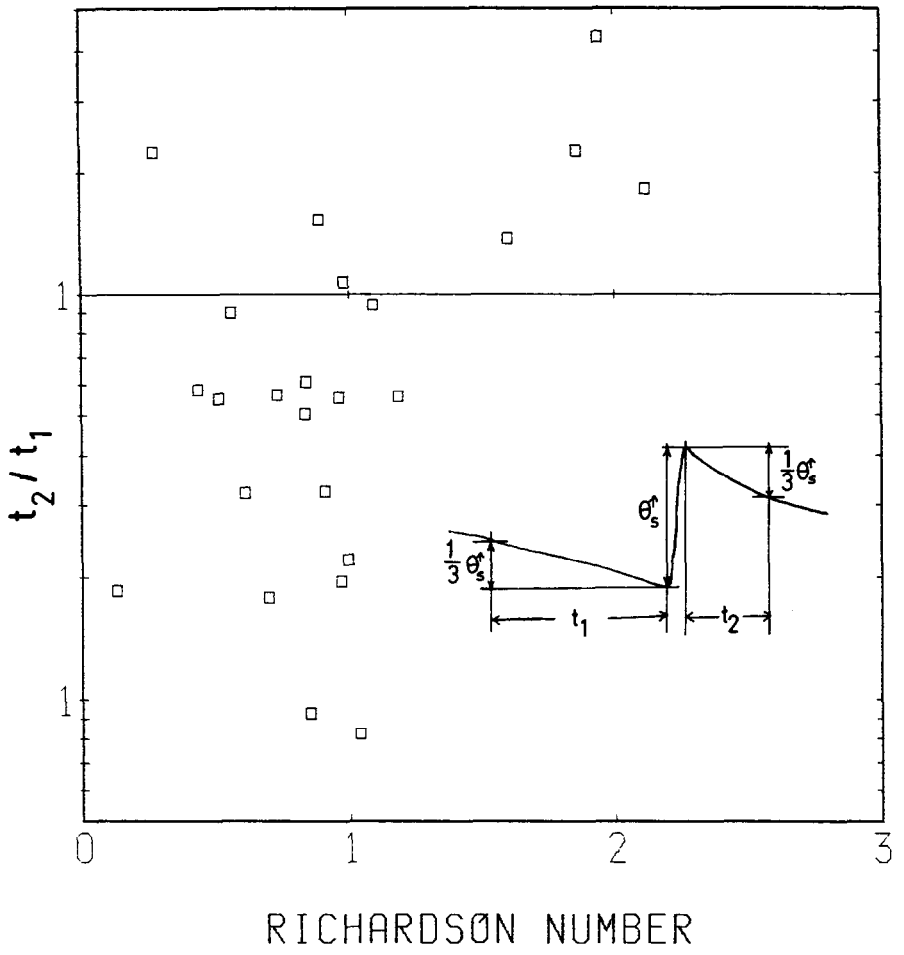

Fig. 6. Comparison of slopes before and after the upward step in terms of the ratio t_2/t_1 plotted against Richardson number. Definitions of t_1 and t_2 are given in the inset. Note that the temperature slopes before and after the step are given by $\theta_s^{\uparrow}/3t_1$ and $\theta_s^{\uparrow}/3t_2$, respectively.

7. Vertical Wind Velocity and Heat Flux in the Inverted Ramp

Figure 7 shows typical examples of the ensemble averages of temperature, $\hat{\theta}$, vertical component of wind velocity, $\hat{w}$, and instantaneous heat flux (divided by the air density and the specific heat under constant pressure), $\widehat{w\theta}$, before and after the upward steps in moderate stability ($R_i = 0.97$). The time-inverted temperature ramp is shown after the temperature step. The corresponding vertical wind shows upward values before the step and downward ones after it. Downward heat flux just after the step is about three times the overall (20-min) average heat flux. Inspection of the other runs in $R_i < 1.5$ shows similar patterns with only a few exceptions.

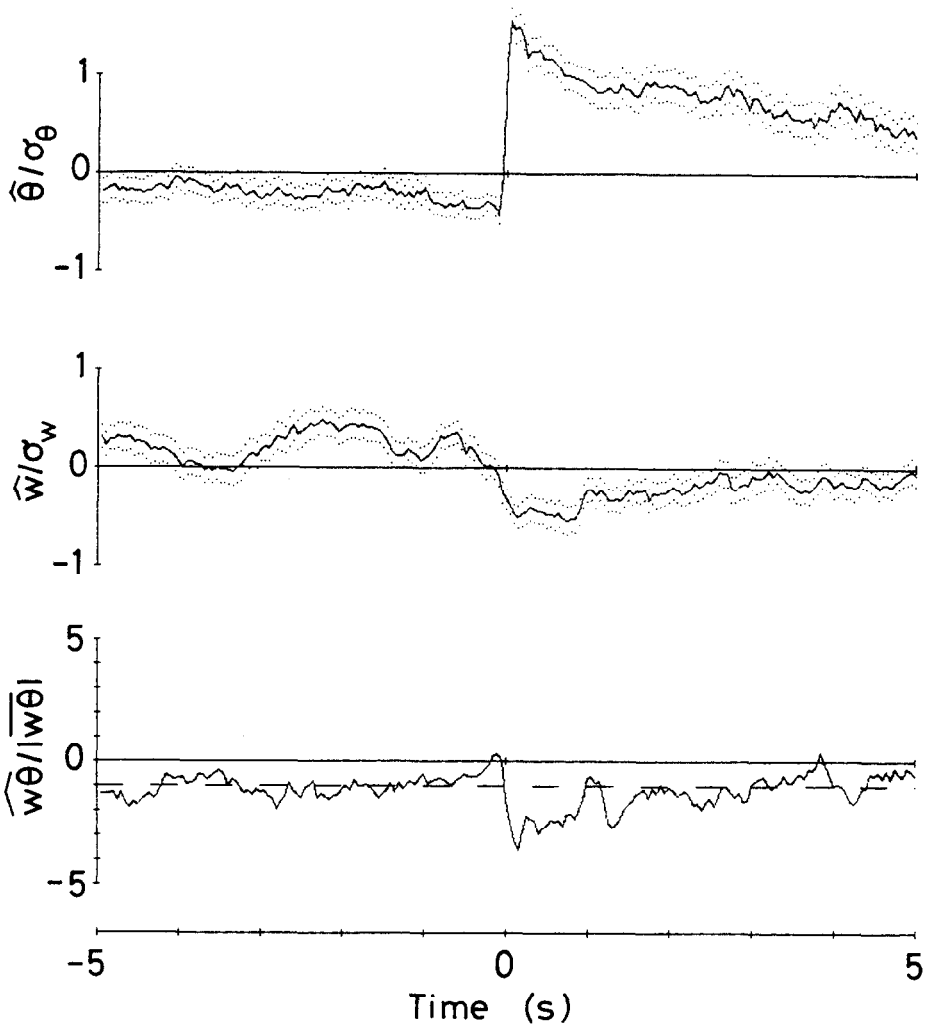

Fig. 7. An example of ensemble averages (a) $\hat{\theta}/\sigma_\theta$, (b) $\hat{w}/\sigma_w$, and (c) $\widehat{w\theta}/|\overline{w\theta}|$ before and after upward steps in moderate stability (R_i = 0.97). Dots in (a) and (b) represent the standard error.

The patterns shown in Figure 7 indicate the presence of descending hot air. Since the buoyant force on the hot air must be directed upward, there must be another force coming from the surrounding air. If this is the result of gravity waves, a likely possibility in stable conditions, the phases of θ and w must differ by $\pi/4$ (Kondo *et al.*, 1978), and there is no reason why the steps should appear only at the cold to hot interface. The only possible mechanism for this time-inverted ramp is related to forced convection, in which temperature plays only a passive role. The upward step can be interpreted as a sharp interface in front of the hot air because descending air has larger horizontal momentum than the surrounding cold air and thus tend to catch up to it.

The contribution of the time-inverted ramp to the total heat flux is calculated as $(Nt_2/t_p)([\overline{w\theta}]_2/\overline{w\theta})$, where N is the number of upward steps detected in the period of

a run, t_p (= 20 min), and $[\overline{w\theta}]_2$ represents the heat flux in Stage 2. The runs with $t_2 > t_1$ have been selected from Figure 6 and the contribution to the total flux has been calculated. The contribution of the heat flux in the inverted ramp ranges between 1.2–17.1% in the range $0.13 < R_i < 1.25$. The resulting value contains considerable scatter and is very small compared with the result obtained by Phong-anant *et al.* (1980) for temperature ramps in unstable conditions. This is partly because the duration of a ramp is underestimated by taking the boundary at $\theta_s^{\uparrow}/3$ and also because the descending hot air moves against the buoyant force in contrast to the heated ascending plumes in unstable air.

On the other hand, Figure 8(1) shows the patterns associated with upward steps in very stable conditions. A temperature-inverted ramp is found and the corresponding vertical wind is upward both before and after the step. Instantaneous heat flux changes sign after the step; thus the temperature ramp does not seem to contribute much to the total heat flux.

Similar features appear on patterns with upward steps as shown in Figure 8(2). In this case, the vertical wind is downward on both sides of the downward step, the heat flux before and after the step cancelling out. The number of downward steps detected in 20 min is 50, which is comparable with 56 upward steps.

These features in very stable conditions indicate the presence of gravity waves in which the phase of temperature and vertical wind differs by $\pi/4$ (Kondo *et al.*, 1978). Since the averaging process involved can blur some features, it is possible that the ramp patterns in Figure 8 do not correspond to the actual wave pattern. In the case of the example shown, the original temperature trace displayed random rectangular waves rather than ramp patterns.

8. Conclusions and Discussion

As already indicated by other workers (e.g., Phong-anant *et al.*, 1980), an upward temperature step related to the inverted ramps occurs in a stable atmospheric surface layer. Normalized frequency of the step as well as normalized peak frequency of the temperature spectrum increases with increasing stability. The normalized magnitude of the temperature step decreases with increasing stability reaching a constant value at $R_i = 1$. These results suggest that step-like temperature fluctuations become more important as stability increases. With respect to the relation between steps and ramps, the time-inverted ramp pattern occurring after the step is found in moderate stability ($R_i \lesssim 1.5$) whereas the steps in strong stability are related to gravity waves.

A closer study of the inverted ramp revealed that descending air and relatively large downward heat flux occurred in the time-inverted ramp, indicating that forced convection plays an important role in creating the inverted ramp. A similar pattern is found in the horizontal component of the wind in laboratory turbulence very near the wall (e.g., Wallace *et al.*, 1977); in that case it is called a 'sweep' pattern. Although the mechanisms involved may be completely different from those in laboratory turbulence, it seems probable that the inverted temperature ramps are related to some ordered structures in

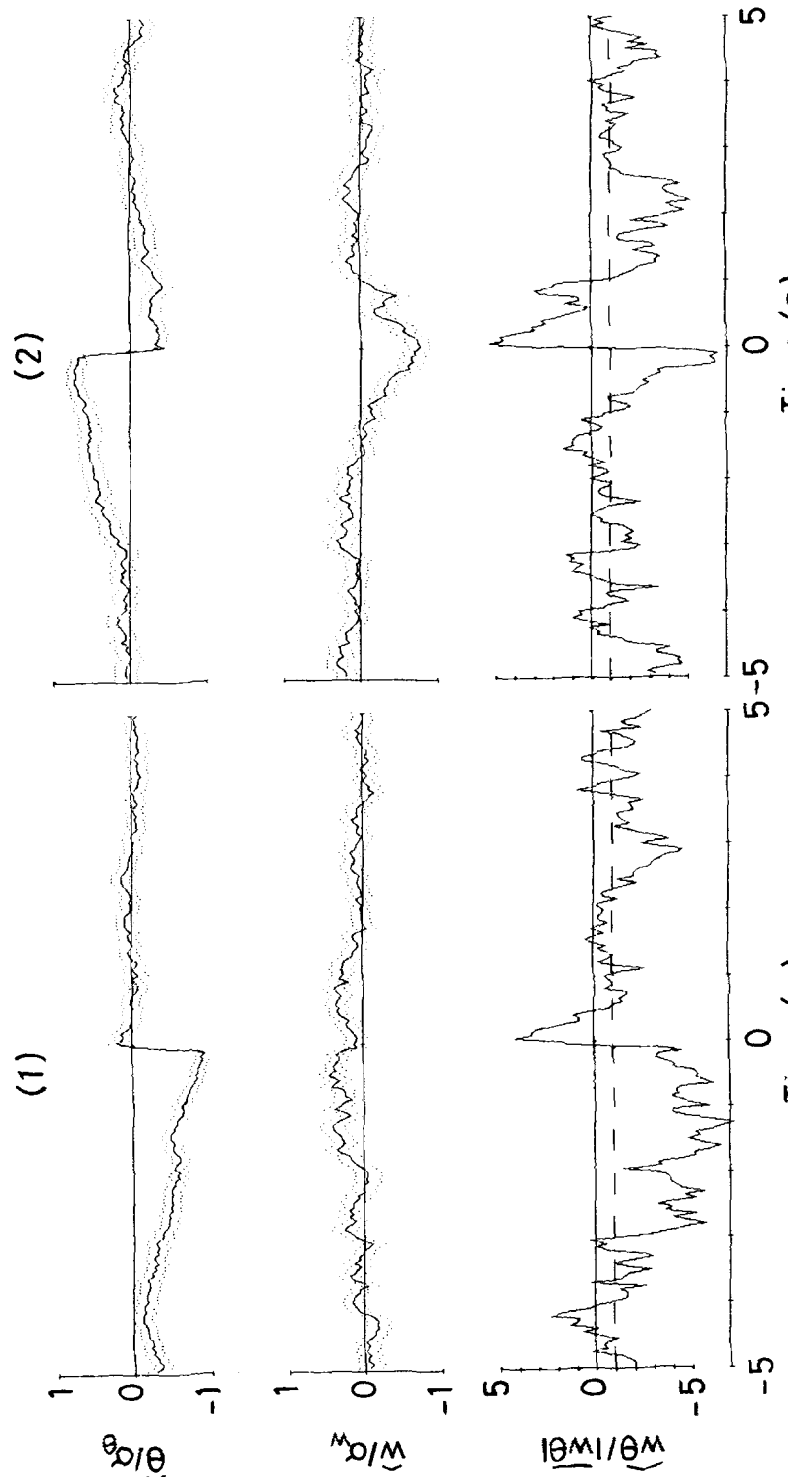

Fig. 8. An example of ensemble averages associated with (1) upward and (2) downward steps in strong stability (R_i = 1.94). Legends are the same as in Figure 8.

the wind. Simultaneous measurements of horizontal wind components would be helpful in explaining the relation.

Acknowledgment

This study was supported by Funds for Scientific Research from the Ministry of Education of Japan.

References

Antonia, R. A., Chambers, A. J., Friehe, C. A., and Van Atta, C. W.: 1977, 'Temperature Ramps in the Atmospheric Surface Layer", *J. Atmos. Sci.* **36**, 99–108.

Antonia, R. A., Rajagopalan, S., and Chambers, A. J.: 1983, 'Conditional Sampling of Turbulence in the Atmospheric Surface Layer', *J. Climate and Appl. Meteorol.* **22**, 69–78.

Chiba, O.: 1984, 'Height Dependence of the Scale of Turbulence and Higher-Order Moments of the Vertical Wind Velocity in the Neutral Atmospheric Surface Layer', *J. Met. Soc. Japan* **62**, 312–322.

Chiba, O. and Kikuchi, T.: 1982, 'A Semiempirical Formula for the Vertical Wind Velocity Skewness in the Unstable Atmospheric Surface Layer', *Tenki* **29**, 1213–1220 (in Japanese).

Kaimal, J. C. and Businger, J. A.: 1970, 'Case Studies of a Convective Plume and Dust Devil', *J. Appl. Meteorol.* **9**, 612–620.

Kaimal, J. C., Wyngaard, J. C., Izumi, Y., and Coté, O. R.: 1972, 'Spectral Characteristics of Surface-Layer Turbulence', *Quart. J. R. Meteorol. Soc.* **98**, 563–589.

Kline, S. J., Reynolds, W. C., Schraub, F. A., and Runstadler, P. W.: 1967, 'The Structure of Turbulent Boundary Layers', *J. Fluid Mech.* **30**, 741–773.

Kondo, J., Kanechika, O., and Yasuda, N.: 1978, 'Heat and Momentum Transfer under Strong Stability in the Atmospheric Surface Layer', *J. Atmos. Sci.* **35**, 1012–1021.

Kovasznay, L. S. G., Kibens, V., and Blackwelder, R. F.: 1970, 'Large-scale Motion in the Intermittent Region of a Turbulent Boundary Layer', *J. Fluid Mech.* **41**, (2) 283–325.

Phong-anant, D., Antonia, R. A., Chambers, A. J., and Rajagopalan, S.: 1980, 'Features of the Organized Motion in the Atmospheric Surface Layer', *J. Geophys. Res.* **85**, 424–432.

Saito, M. and Ishii, Y.: 1969, 'Simple Recursive Filter', *Butsuri-tanko (Geophysical Exploration)* **22**, 527–532 (in Japanese).

Wallace, J. M., Eckelmann, H., and Brodkey, R. S.: 1972, 'The Wall Region in Turbulent Shear Flow', *J. Fluid Mech.* **60**, 39–48.

Wallace, J. M., Brodkey, R. S., and Eckelmann, H.: 1977, 'Pattern-Recognized Structures in Bounded Turbulent Shear Flows', *J. Fluid Mech.* **83**, (4) 673–639.